Columbia University
in the City of New York

LAMONT GEOLOGICAL OBSERVATORY
PALISADES, NEW YORK

Technical Report on Seismology No. 36

Performance of Resonant Seismometers

LAMONT GEOLOGICAL OBSERVATORY

(Columbia University)

Palisades, New York

Technical Report on Seismology No. 36

CU-49-54-AF 19(122)441-GEOL.

Performance of Resonant Seismometers

by

William L. Donn, Maurice Ewing and Frank Press

The research reported in this document has been made possible through support and sponsorship extended by the Geophysics Research Division of the Air Force Cambridge Research Center under Contract AF 19(122)441. It is published for technical information only and does not represent recommendations or conclusions of the sponsoring agency.

May 1954

ABSTRACT

A group of resonant vertical seismometers, each tuned to cover a part of the spectrum of microseism frequencies, has been operated for about one year.

These instruments

(a) clearly distinguish between simultaneous microseisms from two separate sources

(b) show an improved signal-to-noise ratio for microseisms from a single storm, permitting earlier detection of storm onsets

(c) show clearly the increase in period of frontal microseisms as cold fronts move seaward from the east coast of North America

(d) record only the envelope of the oscillations which greatly facilitates measurement of intensity as a function of time.

(e) appear to be very useful tools in continued attempts at hurricane location by means of microseism amplitude studies.

INSTRUMENTATION

The resonant seismographs used in this study consisted of highly underdamped vertical seismometers coupled through a large series resistance to critically damped galvanometers. The seismometers incorporate a design originally suggested by Lacoste (1934) for the use of a zero length spring. Damping of the seismometers and overall sensitivity were controlled by selecting appropriate values for the transducer coil impedance and the series resistance. Leeds-Northrop type 2500F galvanometers (T_g=12-15 sec) were used.

Figure 1 shows the steady state magnification curves for the resonant seismographs. It is seen that each instrument is sharply tuned to a narrow band and that the peak magnification is roughly ten or twenty times greater at these periods than in conventional seismographs. Damping constants for the seismometers are given in Table I.

The magnification curves in Figure 1 are valid only for steady state sinusoidal ground motion. It is well known that microseism amplitudes often change rapidly, a typical variation taking the form of groups containing 3-8 oscillations. Without going into the details we may conclude from the results of Wilson (1932) that the response of tuned seismometers to typical microseisms consists of forced oscillations having the microseism period and slightly damped free oscillations having the period of

the seismometer. The amplitude of the forced vibrations is roughly dependent on the magnification curves of Figure 1 whereas the free vibration amplitudes depend on the amplitude of the spectral components of the transient microseismic activity having periods near that of the seismometer. From comparison of tuned and standard seismograph records we have found that forced vibrations account for the significant amplitude variations of the tuned seismographs and that these are directly related to period and amplitude changes of microseisms.

Table 1

Seismometer Period	Seismometer Damping Constant
2.9 sec	.135 sec^{-1}
4.3	.058
6.3	.019
7.4	.029

PERFORMANCE

The performance of the new instruments can be shown best by a series of case histories of different microseismic situations. Conventional seismograms are illustrated for comparison in many of the cases described below.

November 3-4, 1952

The weather chart (lower right) in Figure 2 shows a weak cold front just east of Palisades (P) at the time indicated. The dotted line off the east coast on this and subsequent charts represents the 1,000 fm. depth contour. The record from the electronic seismograph is shown to the left. This instrument is usually the most sensitive of the Palisades seismographs to short-period microseisms. The earliest detectable microseism signal on this trace occurs about 2230, November 3, with no strong intensity until after 2400. Maximum intensity on this record is from 0100 to 0600, November 4, with the measured period being about 3 sec.

The upper part of Figure 2 reproduces portions of the resonant seismograms having T_o set at 1.5, 2.0, 3.0, 4.5 and 7.0 sec. Each band shown has a duration of 13 hours. A decrease in intensity of the recording light spot is made for 15 minutes every two hours. Owing to the slow drum speed, traces from five seismograms can be recorded on a single drum as shown. Further, the amplitude envelope for a particular frequency can be seen readily, without laborious measurement. The bristle or brush effect results from the compressed time scale and is the signature of the microseism wave groups common on the faster speed records. Since the brush patterns are not usually simultaneous on the several channels, it follows that different signals are being recorded, the difference being essentially one of period.

The resonant seismograms show a succession of events from the 1.5 to the 4.5 sec bands beginning on the former about 2030, November 3, and corresponding in time to the offshore movement of the cold front. Thus, the microseism signal on both the 1.5 and 2.0 sec bands precedes significant activity on the short period electronic seismograph. The maximum intensity is shown on the 3.0 sec channel at the time of maximum intensity on the electronic record, which was measured at 3 sec. The calibration curve for the electronic seismograph shows peak response of 10,000 at 1.7 sec. This suggests that the initial 1.5 to 2.0 sec microseism signal was very weak and that the resonant seismograph is more efficient in detecting such signals when close to the resonant frequency of the instrument. A definite difference in response occurs for microseisms with periods 1/4 to 1/2 octave apart. The increase in microseism period with time and increasing frontal distance (and water depth) is clearly shown by the lower four resonant seismograms.

It is noteworthy that the high noise level on the 7.0 sec band does not affect shorter period channels and is not recorded on the electronic record which still has a magnification of about 2,000 at 7.0 sec.

October 6-8, 1952

Charts A to D in Figure 3 show the progress of close marine and coastal weather events from the middle Atlantic states to Greenland for October 6 to 8, 1952. Charts A and B show a steep pressure gradient

over the ocean area between Labrador and Greenland. This gradient and related high winds weakened considerably during the latter part of October 7. Concurrently, a slowly-moving cold front approached the coast and then passed seaward, crossing coastal waters near Palisades (P) by 1230, October 7.

Resonant seismograms (T_o=1.5, 2.0, 3.0, 4.5 and 6.6 sec) from October 6 at 0900 to October 8 at 1300 are shown in Figure 4. A fairly strong signal is evident on the 4.5 and 6.6 sec bands on the October 6-7 records (upper set). This activity decreases considerably on the lower set of 4.5 to 6.6 sec records for the October 7-8 interval. During the more intense activity on October 6-7, the lines of maximum deflection (giving the brush effect) generally match on the 4.5 and 6.6 sec bands indicating response to the same signal. This is supported by the fact that the measured period on the electronic seismogram for the dominant microseisms during this interval was 5 to 6 sec, or about midway between these resonant frequencies. This long period microseism activity correlates well with the steep pressure gradient over waters east of Labrador and is a frequent occurrence with this weather pattern. The long period microseisms decreased in intensity as the pressure gradient weakened.

The three short period channels (1.5, 2.0, and 3.0 sec) on the lower set of records (October 7-8) show a sequence of increasing microseism activity proceeding from shorter to longer periods, while the long

period microseisms were declining to background level. The amplitude envelopes were drawn on the original records since lines of maximum deflection were too faint to be reproduced. Maximum deflections on the short period bands are not usually simultaneous, suggesting different origin loci for the microseisms of different period. These short period microseisms correlate closely with the passage of the cold front eastward over close coastal waters.

The standard photographic galvanometer seismographs at Palisades were at background during this entire interval. The electronic seismograph showed microseism activity with trends similar to those of the resonant seismometers, but with a lag in short period response.

January 17-18, 1953

Very striking microseism activity is shown on the 5.7 sec trace in Figure 5 with a matching, but much weaker effect on the 6.8 sec band. The 2.0 and 3.0 sec channels are at background indicating that maximum signal strength is probably close to, but somewhat above 5.7 sec. Direct measurement on standard records gives 5.9 to 6.1 sec for the dominant microseisms at this time.

The weather chart in Figure 6 shows a very intense low pressure area between Labrador and the southern tip of Greenland. This cyclone is considered to be the generating area for the microseism storm of Figure 5. The long period microseisms commenced about the time the cold or

western portion of the cyclone traveled out over the deep water area beyond the 1,000 fm line (dotted). Maximum 6 sec microseism intensity was noted in the preceding case with a steep pressure gradient over the same region, and similar relationships have been observed for many other such situations.

November 5-6, 1952

A marked increase in signal strength occurs toward the end of November 5, on the 7.0 sec channel in Figure 7. These microseisms declined to a fairly constant although high intensity level by 0500 of November 6. The 3.0 and 4.5 sec traces show a continuously high level during the interval and with a definite but slight increase (more marked on the latter) as the 7 sec microseisms decreased. Microseism period measured on standard records during the interval of maximum intensity was 6.0 to 6.5 seconds with a decrease to 5-5.5 sec following maximum. The latter probably explains the increase in signal on the middle channels as intensity decreased on the upper (7 sec) channel. The 1 and 2 sec bands are conspicuously quiet during this interval.

The related weather is shown on the four charts of Figure 8, which illustrate rather typical progress and intensification for this region of the low pressure area indicated. Acoording to the chart at 1230, November 5, the cyclone, although of moderate intensity, extended from deep water northward to the coast. The storm strengthened considerably

in the next six hours as it became smaller and more circular with approach to the coast. Simultaneously, the long period microseism signal (Figure 6) began to increase, and reached maximum strength when the storm center and area of maximum wind velocity was just at the edge of the continental shelf. The storm intensified further as it moved almost completely over the shelf by November 6 at 0630. During this latter interval long period microseisms decreased while the shorter period signal increased somewhat. The steep pressure gradient which persisted eastward from Newfoundland as the central area of the cyclone moved northward over land appears to explain the continuing broad microseism spectrum after the interval of maximum intensity.

Since the short period microseism signal (3.0-4.5 sec) was relatively uniform, it is concluded that it was generated over the shelf zone both preceding and following the passage of the central area of the cyclone. The slight increase in intensity corresponding to the time of passage of the intense central area of the cyclone over the shelf also supports this view. The generation of the intense long period microseisms seems to be related to the position of the cyclone when adjacent to or at the edge of the shelf.

It seems noteworthy that the cyclone traveled almost due north along the 55th meridian. From this fact, and the pattern of wind-flow deduced from the isobars, it seems unlikely that transposition of the two main

fetches (north in the west portion and south in the east portion) could have occurred. Thus the possibility of microseism generation through ocean wave interference in this case seems doubtful.

November 18-19, 1952

The three weather charts in Figure 9 show the intensification of a cyclonic area in much the same position as in the previous case. Note, however, that the storm is practically stationary over the 36-hour interval. This appears to preclude the possibility of wave interference resulting from the transposition of wave fetch. Between 1830 November 18 and 0630 November 19 the area of maximum wind increased as the intensity in the central zone diminished somewhat.

Microseism period measured on the Palisades (Columbia) vertical seismogram: T_o=12, T_g=15 (lower right) increased to 8.5 sec by 0600, November 19, the time of maximum cyclone area.

Resonant seismograms (T_o=1.0, 2.0, 3.0, 4.5 and 7.0) for November 17-19 are reproduced in the two sets of records in Figure 10. Maximum signal strength shows on the 7.0 sec band from 1400 November 18 to 0200 November 19, coinciding with the time of 7 sec microseisms on the standard seismogram. As period increased to 8.5 sec signal strength on the 7.0 sec band decreased.

As in the preceding case, maximum microseism activity appears to be related to the proximity of the generating area to the edge of the

continent as indicated by the 1000 fm contour. It may also be significant that microseisms of longer period 6.5 to 8.5 sec are associated with the two storms south of Newfoundland, whereas shorter periods are associated with the two storms between Labrador and Greenland. The straight isobar pattern occurring with the latter storms would be expected to provide much greater fetch for the development of long period ocean waves than would the more circular pattern of the cyclone south of Newfoundland. It may be relevant to note that a rather limited deep zone exists about 42°N between 50° and 65°W. Bathymetric charts indicate a depth of more than 2900 fm and recent seismic refraction indicates that about 2 km of sediments makes up the bottom. This may well be related to the relatively long period of the microseisms generated in this region.

March 29-30, 1953

Note that in Figure 11, the lowermost trace is for the longest period, in this case (8.0 sec). Following upwards in order, T_o=2.0, 3.0, 4.5 and 6.7 sec. The 8 sec channel shows a very strong signal commencing about 1600, March 29 and continuing for the duration of the record, with maximum strength between 2200, March 29 and 0800, March 30. The quiet 6.7 sec band indicates the lower limit of the spectrum and suggests that peak period is longer than 8 sec. The increasing signal on the 2, 3 and 4.5 sec channels is therefore related to a different microseism source.

Reproductions of the vertical component records from the Palisades (Columbia) and Benioff seismographs are shown in "B" and "C" respectively. The measured period of the dominant microseisms (which are poorly recorded by the Benioff) is 8.5 to 9 sec. This long period signal which is not detectable until 1900 on B and 2200 on C is clearly preceded by the signal beginning at 1600 on the 8.0 sec resonant channel. Also, although the 8 sec intensity continues at more than one-half maximum following 0800 on March 30, the long period microseisms become masked by increase in short period microseisms after 0800, on the standard records (B and C).

The long period 8.5 to 9.5 sec microseisms are correlated with an intense low pressure system off the southern coast of Alaska. Ground particle trajectories which have been constructed for the horizontal plane for these microseisms give elongated orbits whose azimuths coincide with the azimuth of the storm. This has been determined to be a rather frequent occurrence although the microseisms are often masked by more intense shorter period microseisms from Atlantic storms. The short period microseism storm becoming prominent during March 30 has been correlated with a close Atlantic cyclone. The records from the resonant seismometers clearly distinguish between the two microseism storms and permit the study of the amplitudes as a function of time without interference of the separate signals.

August 14-15, 1953 (Hurricane "Barbara")

The track of Hurricane "Barbara", 1953 is shown in Figure 12 together with a plot of Palisades microseisms showing amplitudes as a function of storm position as well as of time. Note that the hurricane center was well on the continental shelf for most of its path.

Figure 13 reproduces records from the three resonant seismometers in operation at the time for which T_o=3.0, 4.0 and 6.0 sec. Maximum signal strength is shown by the 3 and 4 sec channels which show essentially simultaneous beginnings and maxima. Period on standard seismograms was measured at 3.5 to 4 sec. The 6 sec band differs in that the signal appears much weaker and begins about two hours later.

In previous cases (in this report and elsewhere) microseism period increased or decreased when generating areas moved transverse to the continental shelf. As water depth increased uniformly over the shelf a direct relationship between depth and period was suggested. In the present case water depth beneath the hurricane track is essentially constant during the interval of Palisades microseism activity. These observations are in harmony with a depth-period effect.

The microseism-generating area of the hurricane was broader than the narrow center path and actually extended from the coast out to deep water just beyond the shelf. The weak signal on the 6 sec channel is explained as the response to the 4 to 5 sec microseisms that are usually

recorded from wind systems over the deeper water zone. The response is weak in part from being out of resonance with the signal, and in part from the small portion of the hurricane that existed over the deeper water. If the microseisms were generated by ocean waves arriving locally, it would be expected that the longer period response should have occurred earliest, which is not observed here.

CONCLUSIONS

The study of many case histories of microseism storms having varied generating sources and locations indicates that the resonant seismometers

(1) Have an improved signal-to-noise ratio which permits either earlier detection of microseism storms or detection of microseisms which may not otherwise be known to exist;

(2) Permit distinction between simultaneous microseisms from different sources;

(3) Show progressive increase in period of frontal microseisms as fronts move seaward from the eastern coast of North America;

(4) Show definite differences in period characteristics among certain regions of microseism generation;

(5) Permit quick determinations of microseism intensity as a function of time, and show clearly the spectral distribution of microseism energy; and

(6) May, as a result of the above qualities, be a valuable tool in any continued study of hurricane location by means of microseism amplitude comparisons; this is of particular value when simultaneous storms are present, a very frequent occurrence in the Gulf of Mexico and Caribbean area.

ACKNOWLEDGMENTS

We gratefully acknowledge the contributions of Bernard Luskin in the initial design and construction of the seismometers and Harold Smith in their installation and maintenance.

REFERENCES

L. J. B. Lacoste, Jr., A new type long period vertical seismograph, Physics, Vol. 5, pp. 178-180, 1934

H. A. Wilson, The calculation of the motion of the ground from seismograms, Physics, Vol. 2, pp. 84-97, 1932

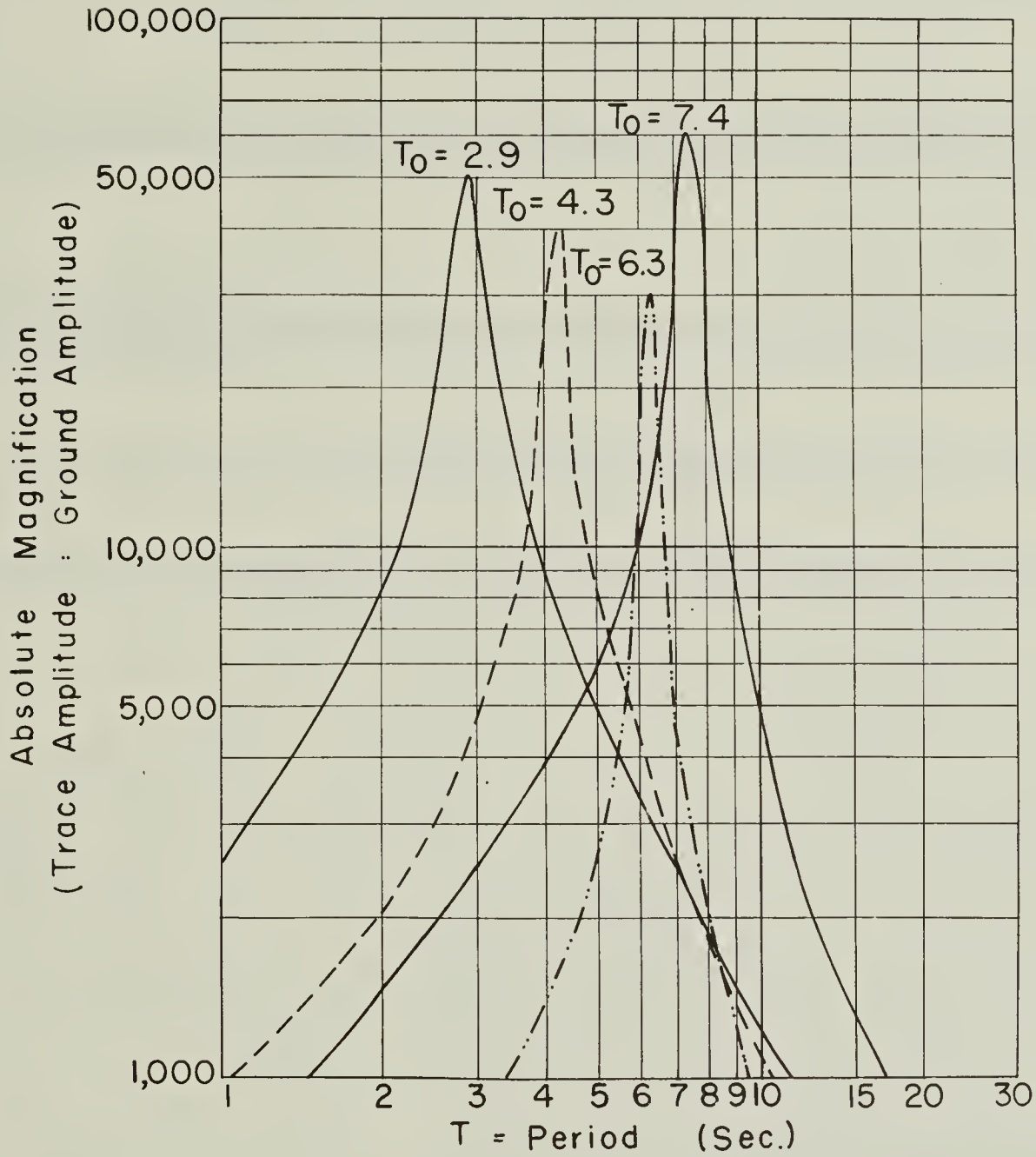
100,000
50,000
10,000
5,000
1,000
Absolute Magnification
(Trace Amplitude ÷ Ground Amplitude)
T_0 = 2.9
T_0 = 4.3
T_0 = 6.3
T_0 = 7.4
1
2
3
4
5
6
7
8
9
10
15
20
30
T = Period (Sec.)

FIGURE 1

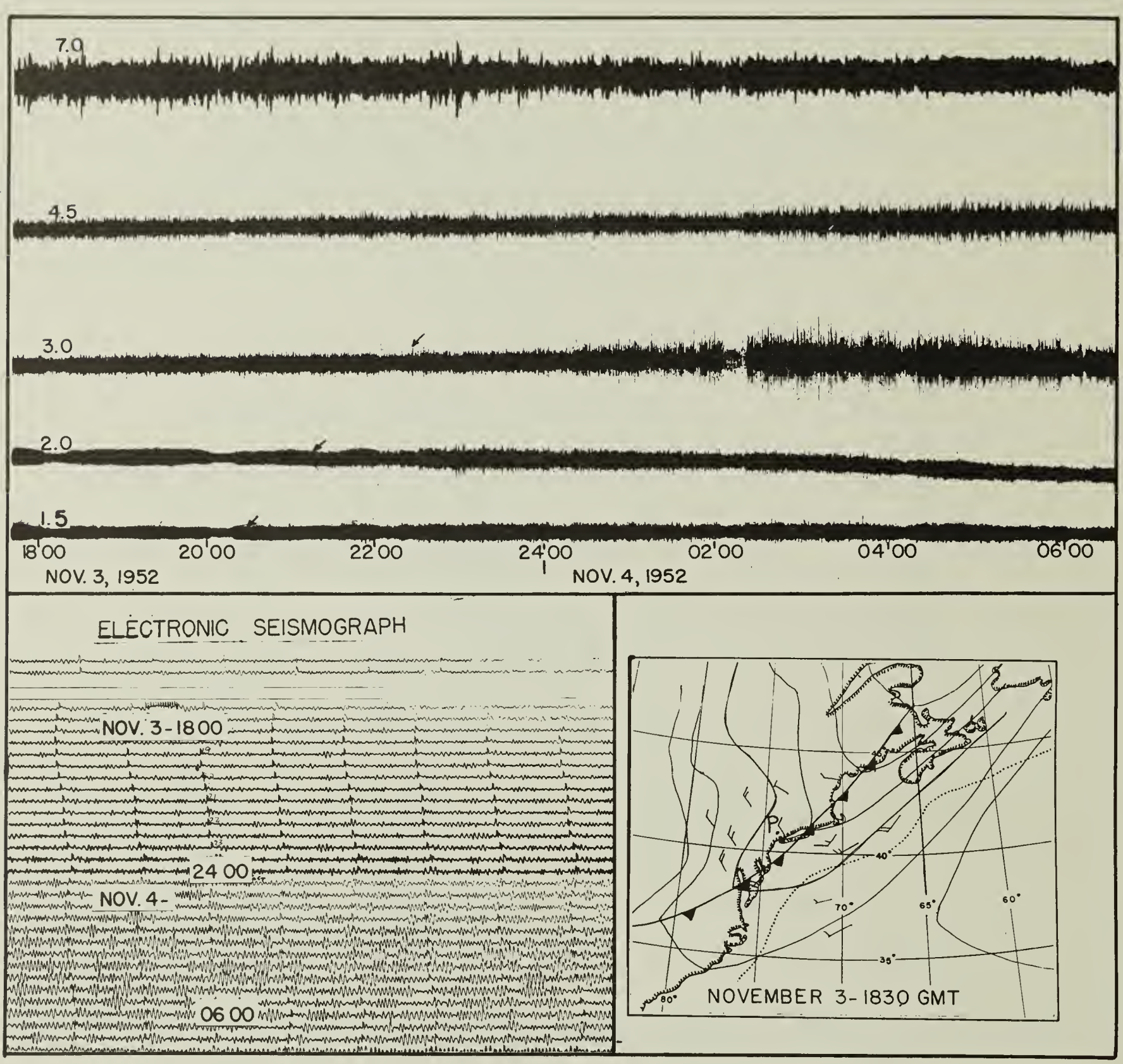
7.0
4.5
3.0
2.0
1.5
18'00
20'00
22'00
24'00
02'00
04'00
06'00
NOV. 3, 1952
NOV. 4, 1952
ELECTRONIC SEISMOGRAPH
NOV. 3-1800
24 00
NOV. 4-
06 00
NOVEMBER 3-1830 GMT

FIGURE 2

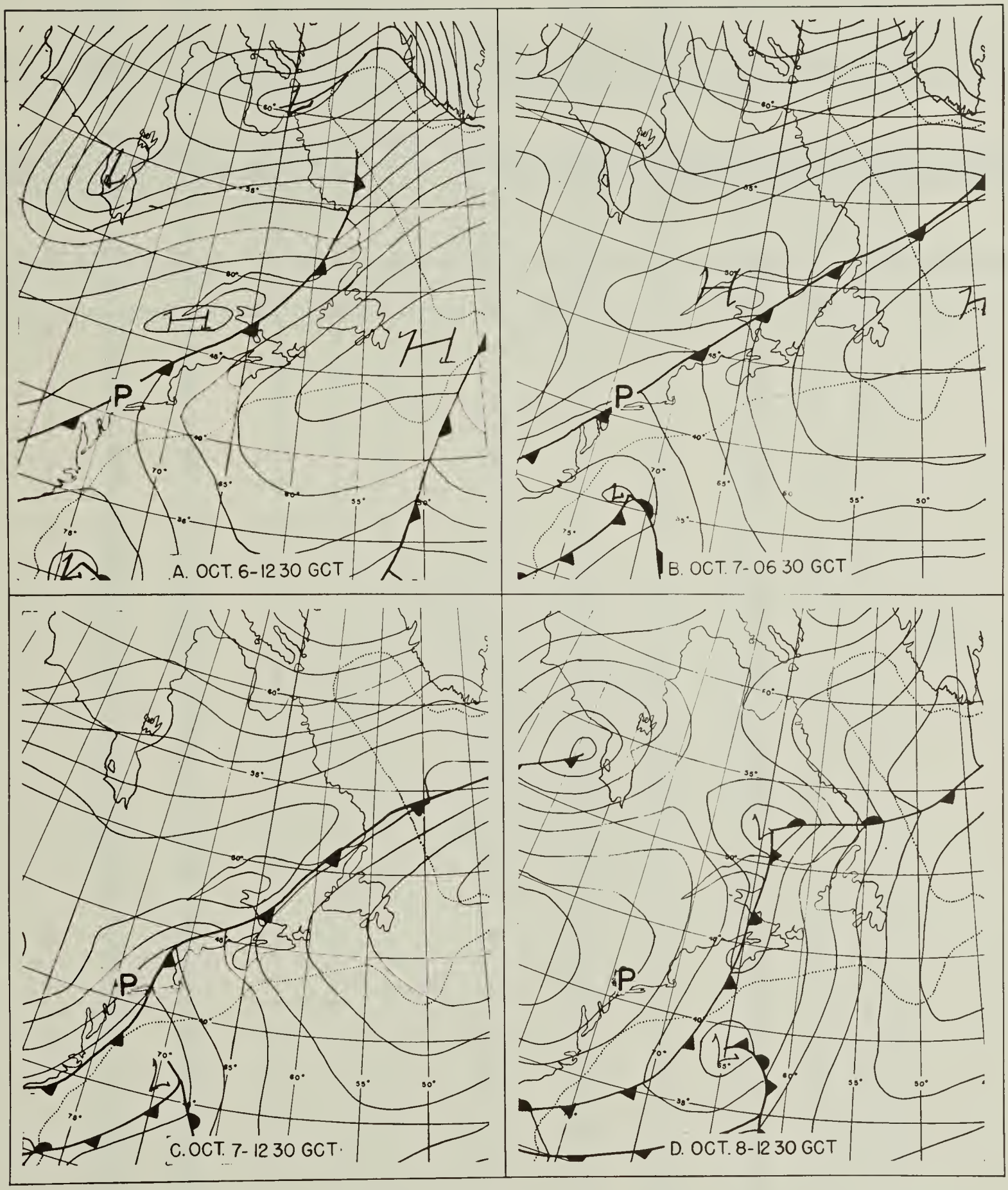

FIGURE 3

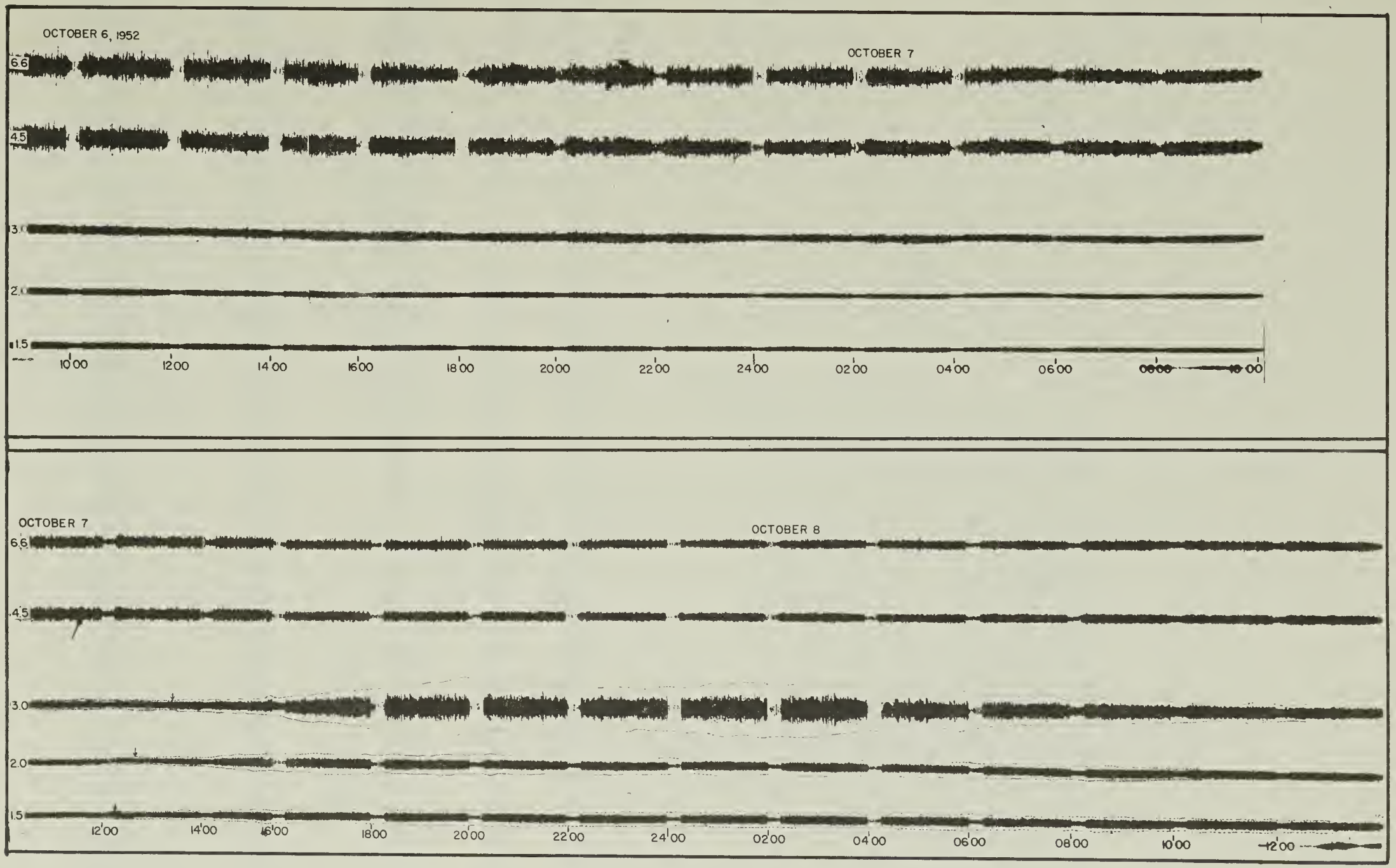
OCTOBER 6, 1952
OCTOBER 7
6.6
4.5
3.0
2.0
1.5
10'00
12'00
14'00
16'00
18'00
20'00
22'00
24'00
02'00
04'00
06'00
08'00
10'00
OCTOBER 7
OCTOBER 8
6.6
4.5
3.0
2.0
1.5
12'00
14'00
16'00
18'00
20'00
22'00
24'00
02'00
04'00
06'00
08'00
10'00
12'00

FIGURE 4

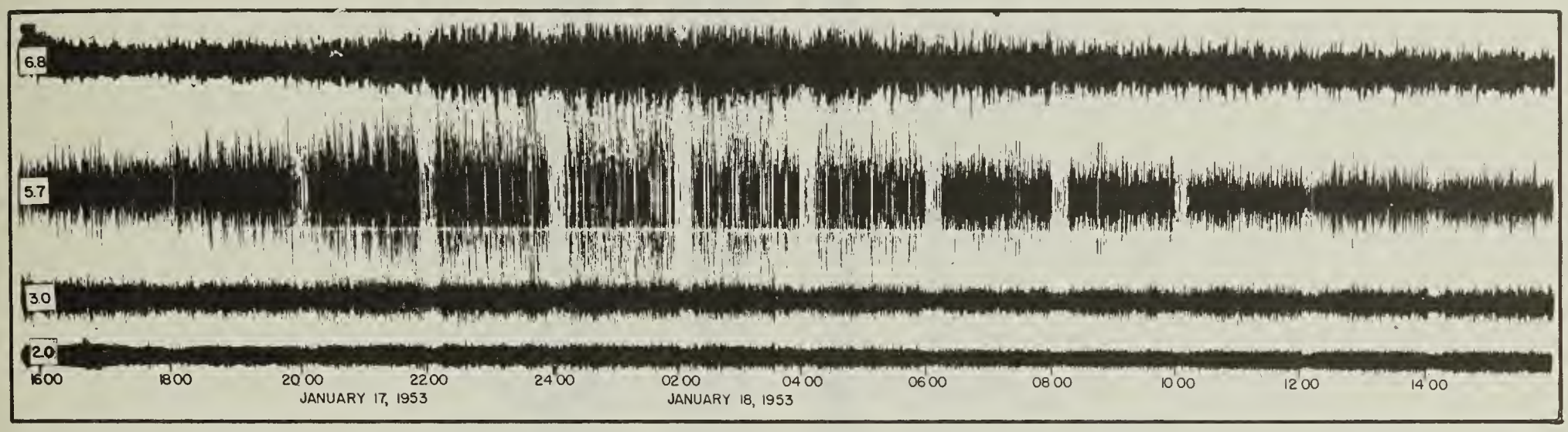

FIGURE 5

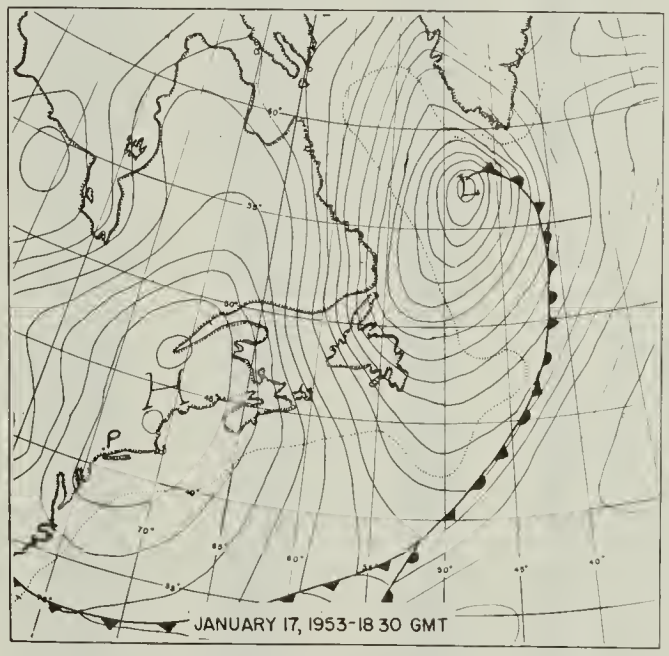

FIGURE 6

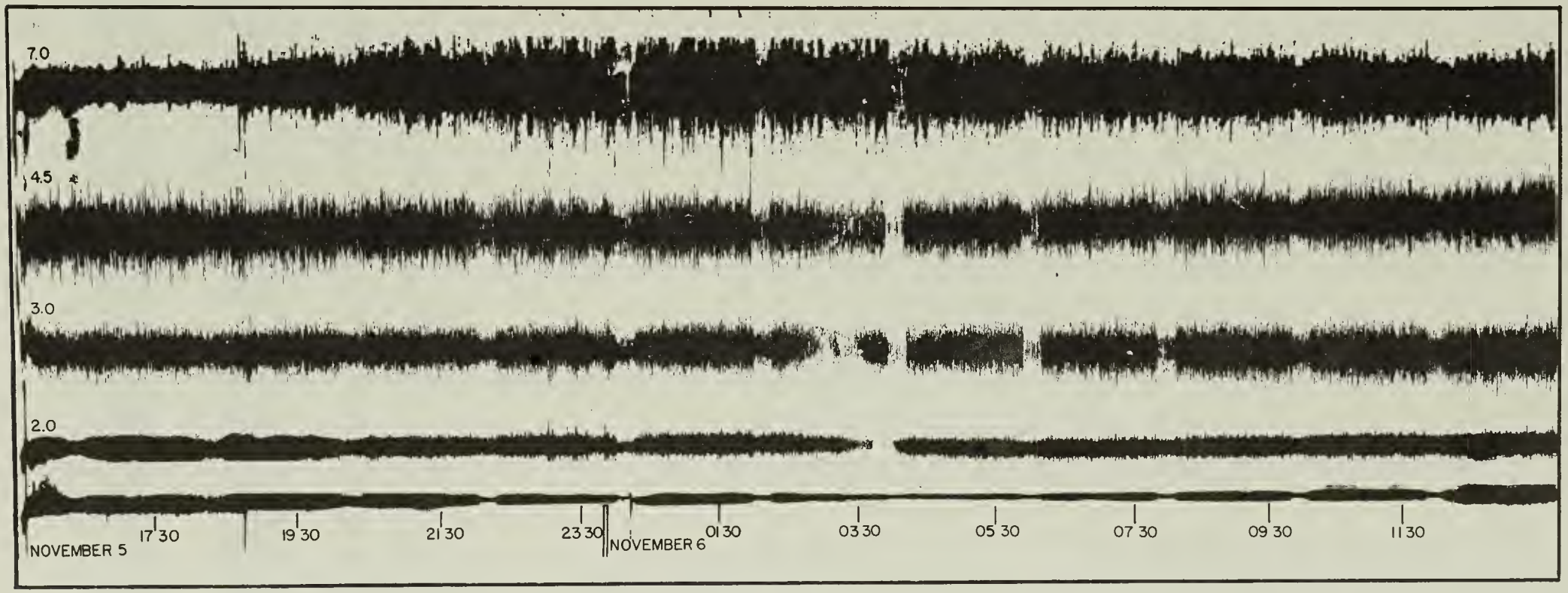
7.0
4.5
3.0
2.0
1.5
NOVEMBER 5
17 30
19 30
21 30
23 30
NOVEMBER 6
01 30
03 30
05 30
07 30
09 30
11 30

FIGURE 7

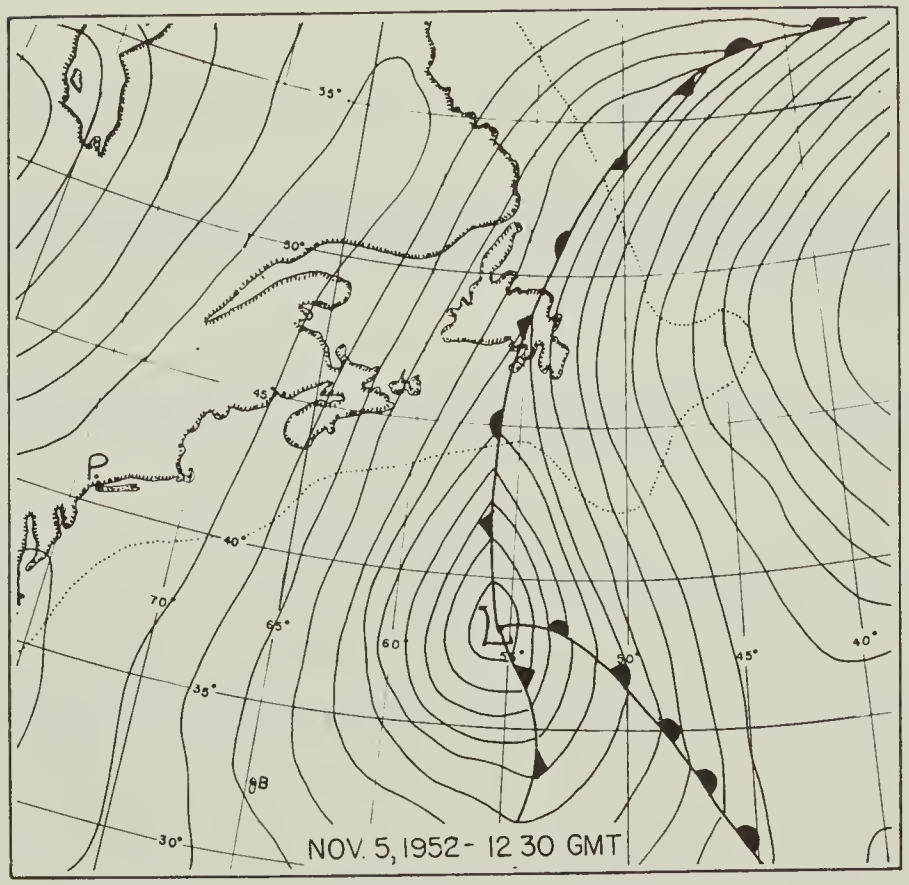
NOV. 5, 1952 - 12 30 GMT

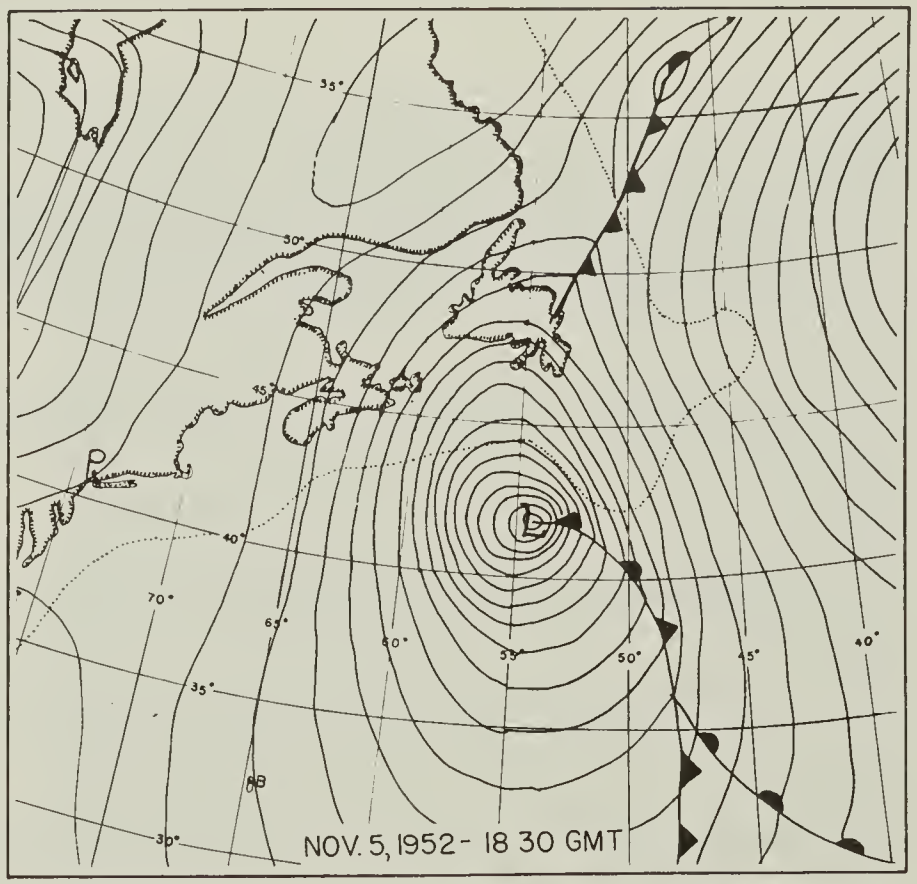
NOV. 5, 1952 - 18 30 GMT

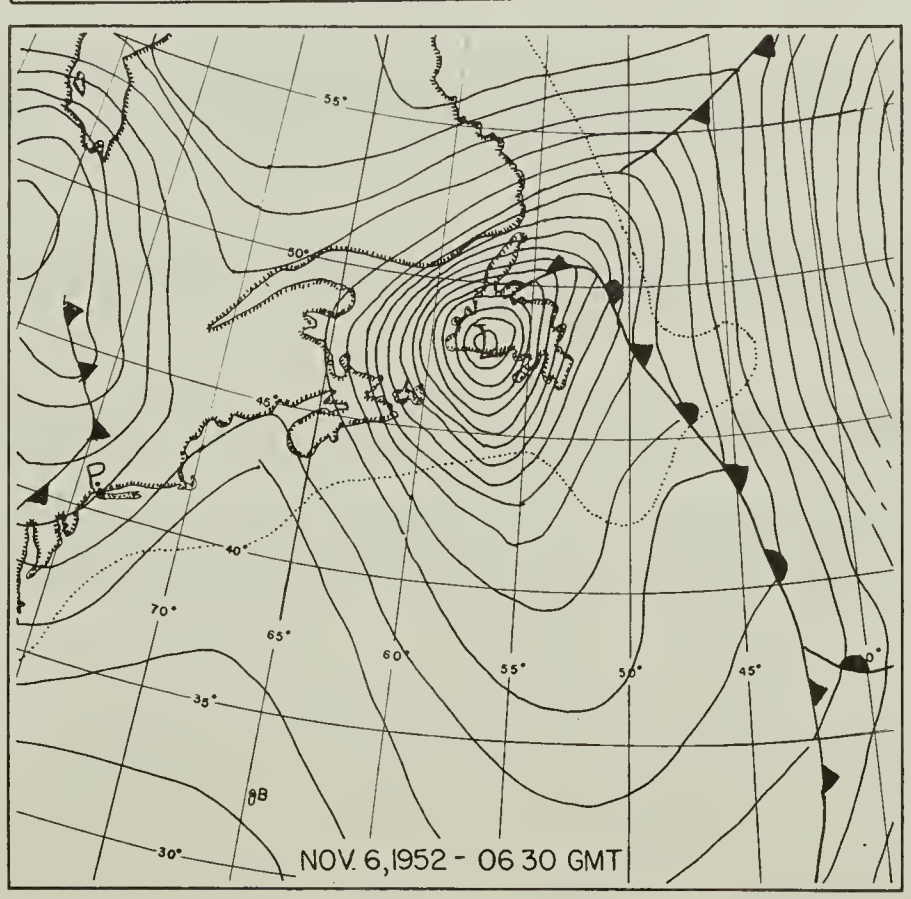
NOV. 6, 1952 - 06 30 GMT

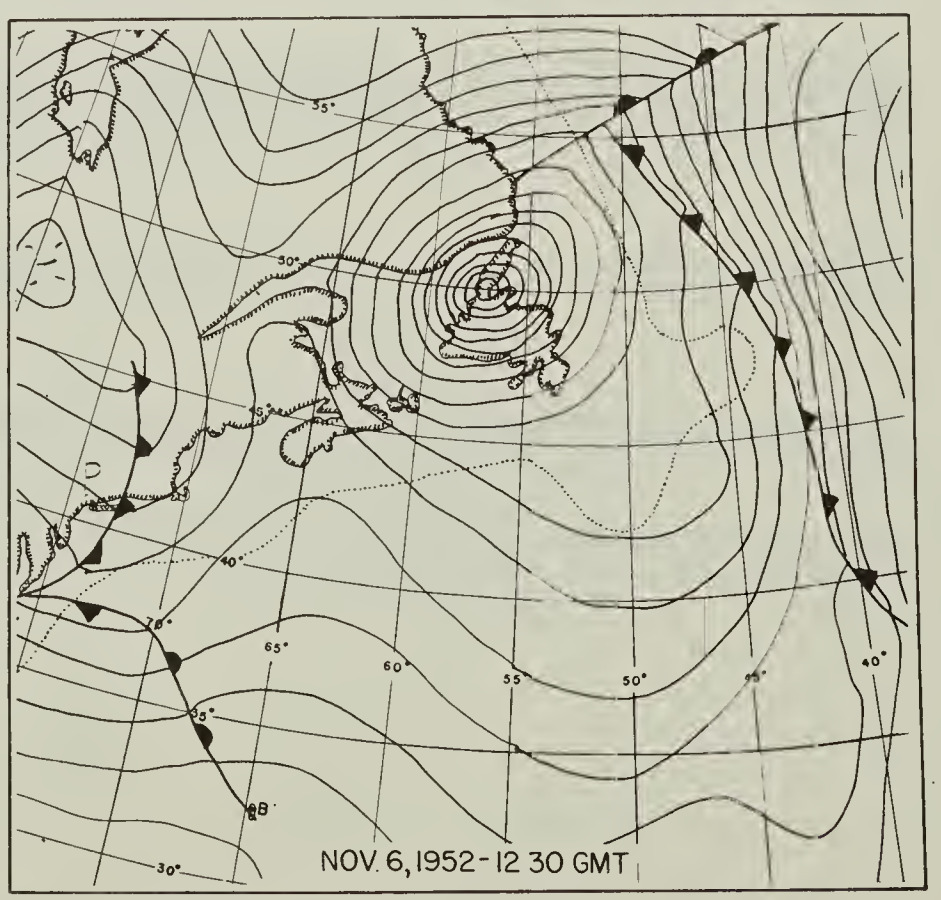
NOV. 6, 1952 - 12 30 GMT

FIGURE 8

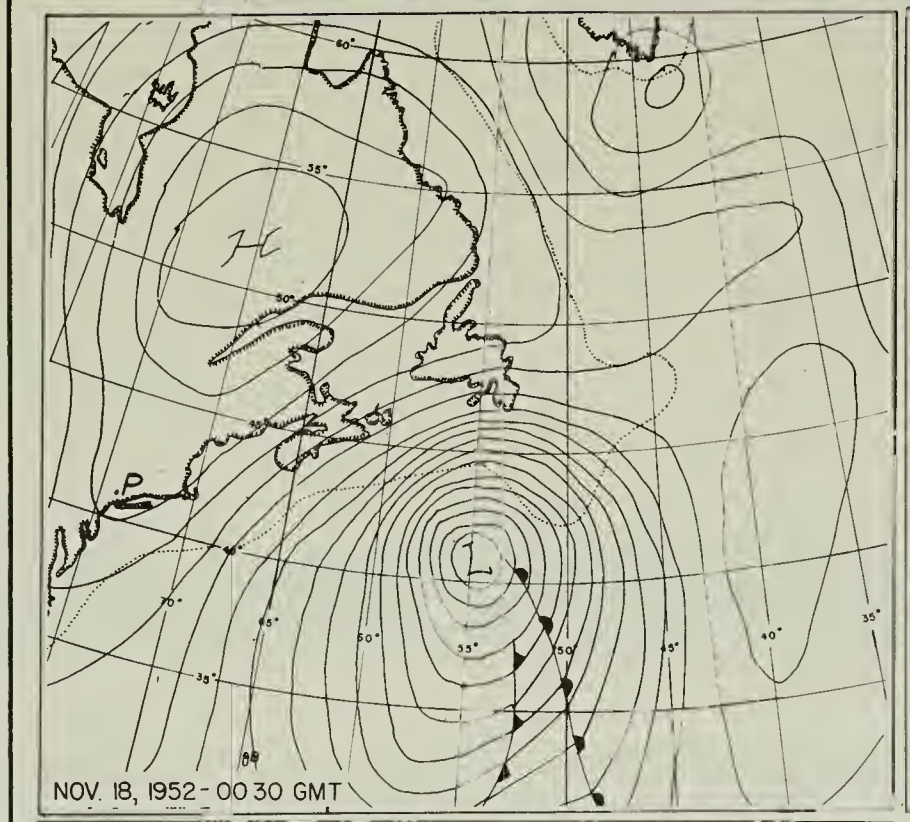
NOV. 18, 1952 - 00 30 GMT

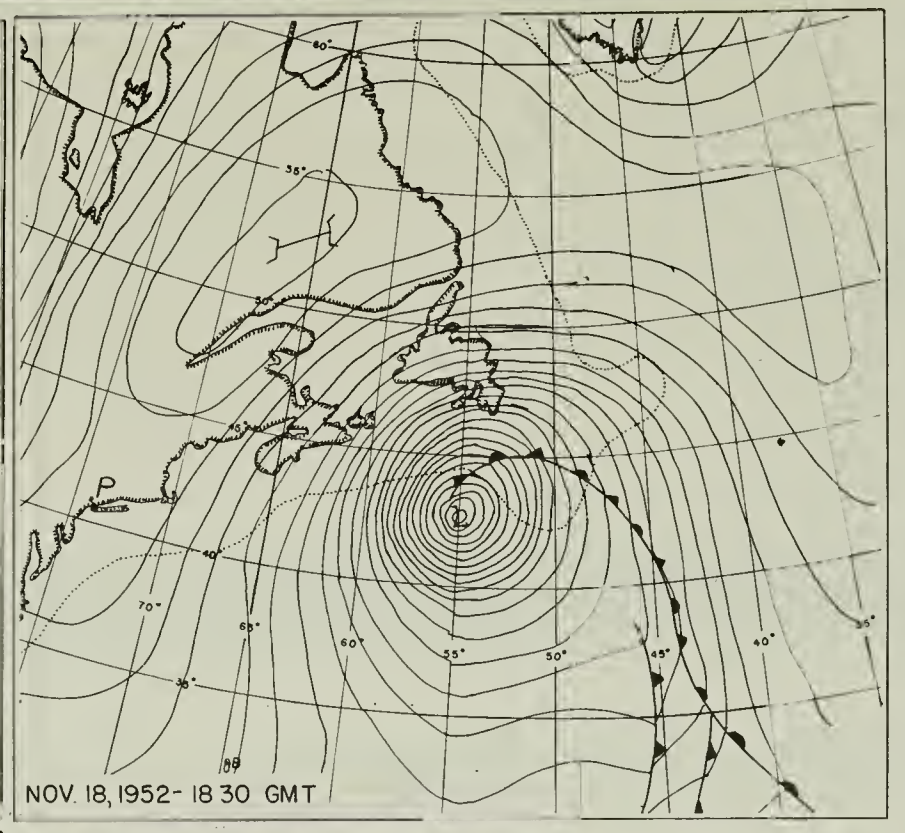
NOV. 18, 1952 - 18 30 GMT

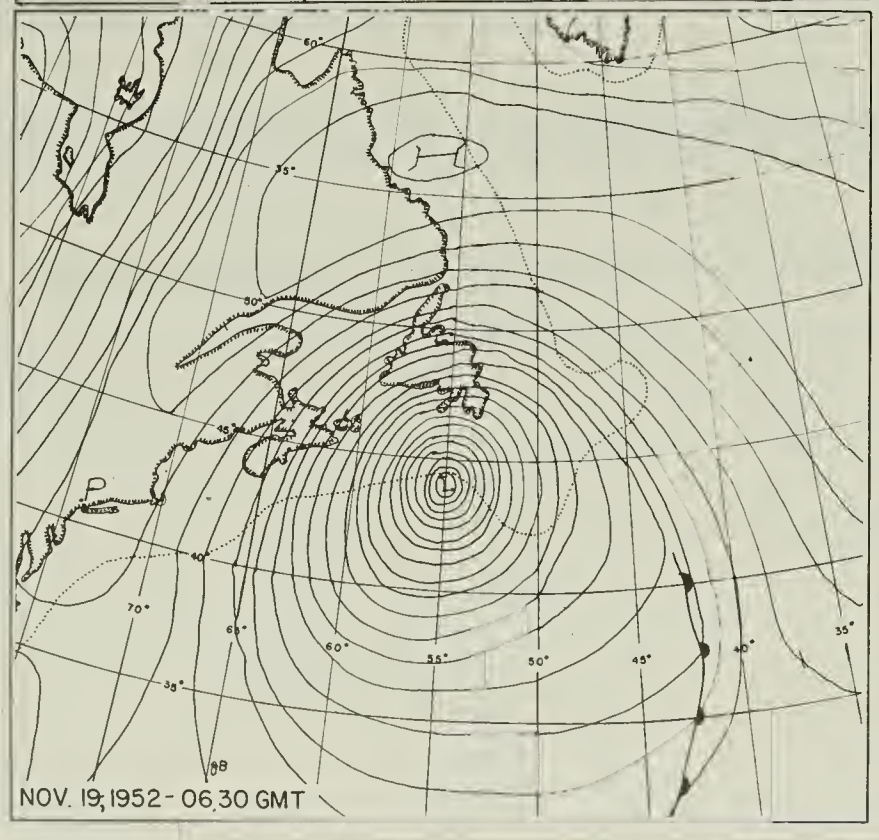
NOV. 19, 1952 - 06 30 GMT

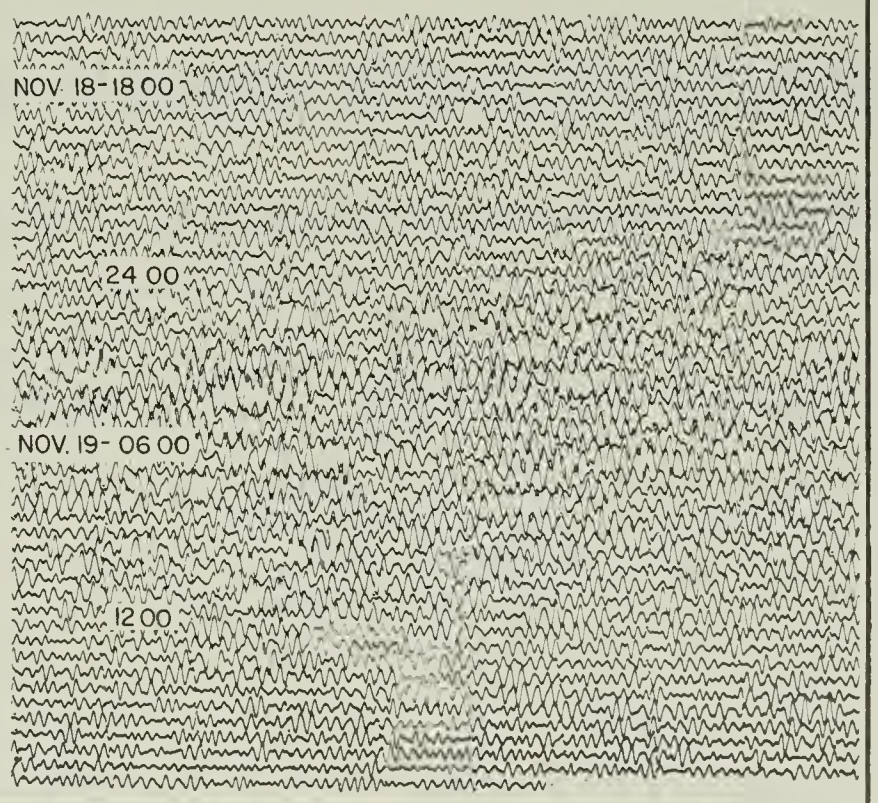
NOV. 18 - 18 00
24 00
NOV. 19 - 06 00
12 00

FIGURE 9

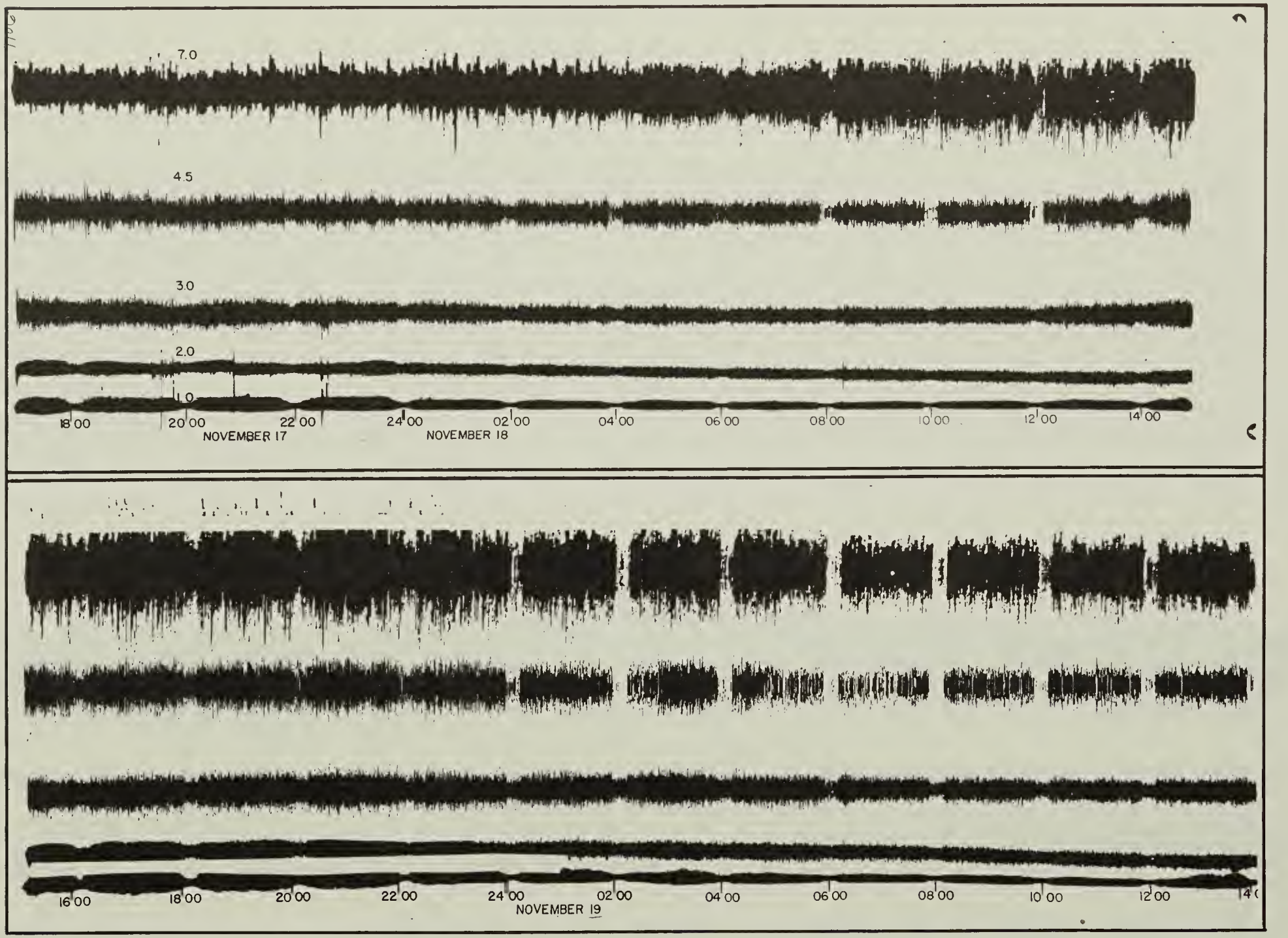
7.0
4.5
3.0
2.0
1.0
18 00
20 00
22 00
24 00
02 00
04 00
06 00
08 00
10 00
12 00
14 00
NOVEMBER 17
NOVEMBER 18
16 00
18 00
20 00
22 00
24 00
02 00
04 00
06 00
08 00
10 00
12 00
NOVEMBER 19

FIGURE 10

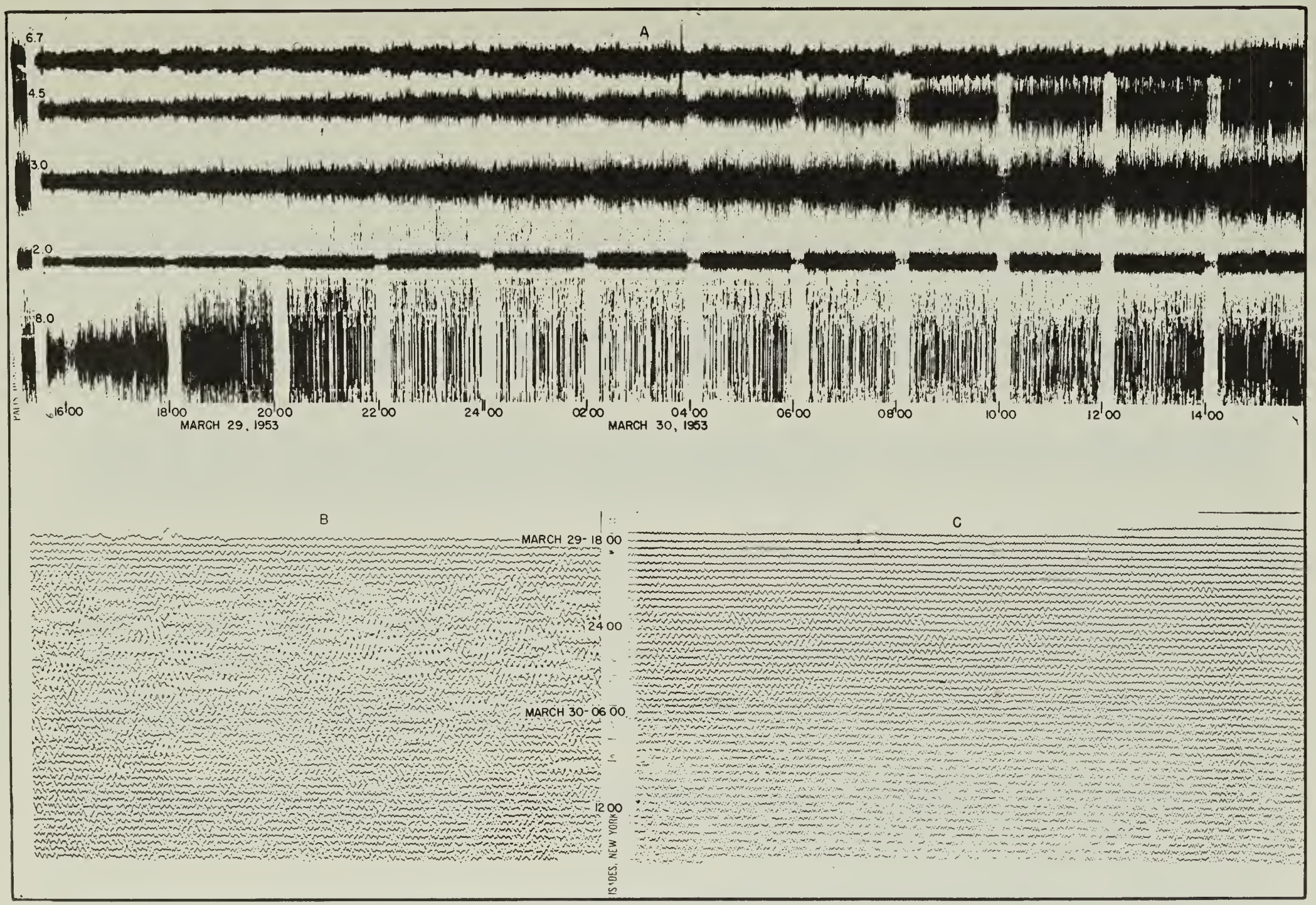
A
6.7
4.5
3.0
2.0
8.0
16 00
18 00
20 00
22 00
24 00
02 00
04 00
06 00
08 00
10 00
12 00
14 00
MARCH 29, 1953
MARCH 30, 1953
B
C
MARCH 29- 18 00
24 00
MARCH 30- 06 00
12 00
ISIDES, NEW YORK

FIGURE II

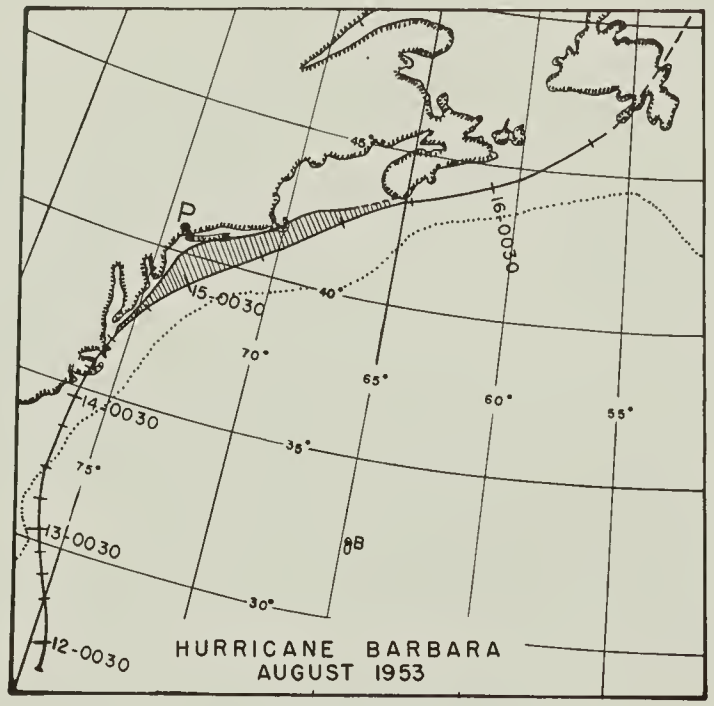

FIGURE 12

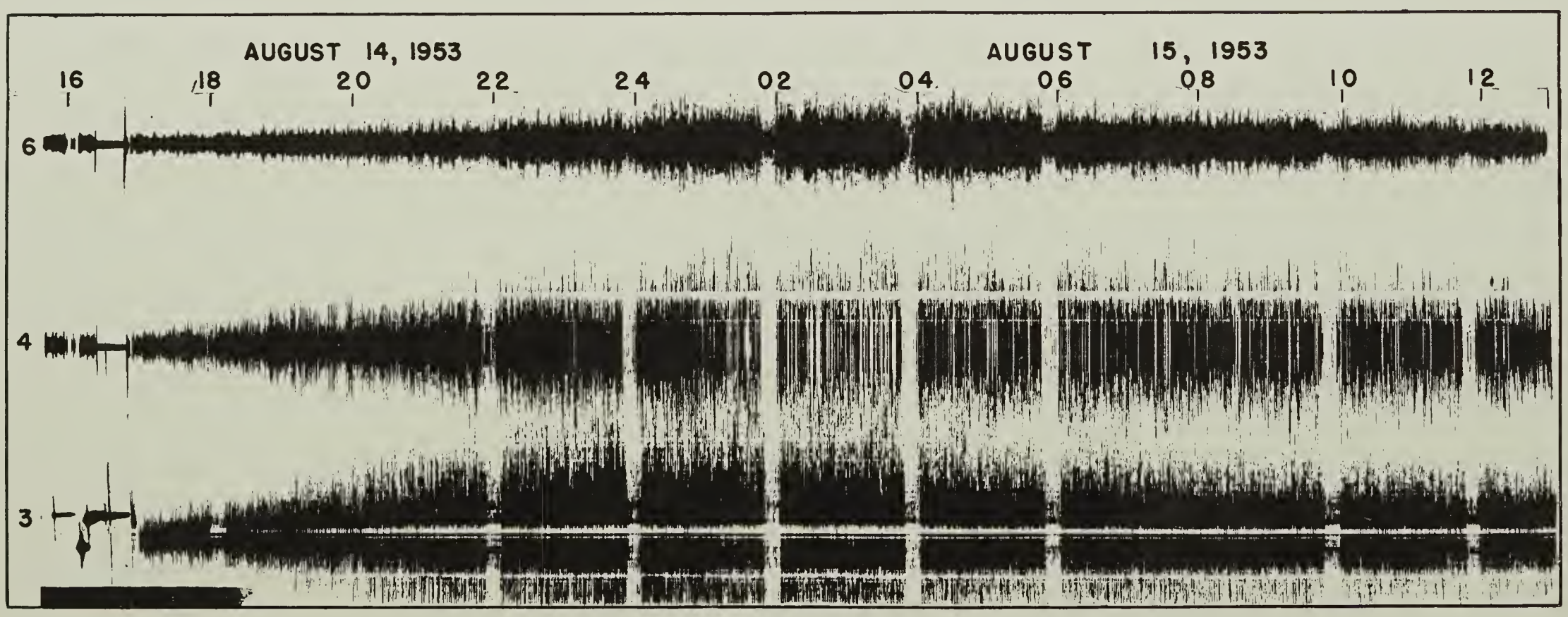

FIGURE 13